

Impact of carrier frequency offset and in-phase and quadrature imbalance on the performance of wireless precoded orthogonal frequency division multiplexing

Suyoto¹, Agus Subekti¹, Arief Suryadi Satyawan^{1,2}, Nasrullah Armi¹, Chaeriah Ali Wael¹, Galih Nugraha Nurkahfi¹

¹Research Center for Telecommunication, National Research and Innovation Agency, Bandung, Indonesia

²Electrical Engineering Department, Faculty of Engineering, Nurtanio University, Bandung, Indonesia

Article Info

Article history:

Received Jul 28, 2021

Revised Apr 19, 2022

Accepted May 14, 2022

Keywords:

Bit error rates

Carrier frequency offset

In-phase and quadrature imbalance

Precoded orthogonal frequency division multiplexing

Signal-to-interference noise ratio

ABSTRACT

Precoding in orthogonal frequency division multiplexing (OFDM) system proved to reduce the peak-to-average power ratio (PAPR), so that it improves BER. However, from the existing literature, the effect of carrier frequency offset (CFO), in-phase and quadrature (IQ) imbalance on precoded wireless OFDM systems has not been carried out. Therefore, this study evaluated the precoded OFDM (P-OFDM) system performance by considering the impact of CFO and IQ imbalance. P-OFDM performance evaluation is expressed in signal-to-interference noise ratio (SINR) and bit error rates (BER). The communication channels used are the additive white Gaussian noise (AWGN) channel and the frequency-selective Rayleigh fading (FSRF) channel, while the channel equalization process is considered perfect. The results of the analysis and simulation show that P-OFDM is greater affected by the presence of CFO and IQ imbalance than conventional OFDM system. In AWGN channel, P-OFDM experiences different SINR for each subcarrier. This is different from conventional OFDM system, where all SINRs are the same for all subcarriers. In the FSRF channel, both the P-OFDM system and the OFDM system experience different SINR for each subcarrier, where the SINRs fluctuation in the P-OFDM system is much larger than in the OFDM system.

This is an open access article under the [CC BY-SA](https://creativecommons.org/licenses/by-sa/4.0/) license.



Corresponding Author:

Suyoto

Research Center for Telecommunication, National Research and Innovation Agency

Building 20. 4th floor St. Cisitua No.21/154D Bandung 40135, Indonesia

Email: suyo004@brin.go.id

1. INTRODUCTION

Orthogonal frequency division multiplexing (OFDM) is still getting attention in wireless communication systems. This is because OFDM has the ability to face inter-symbol interference (ISI) in multipath channels. ISI can be avoided by using cyclic prefix (CP) [1], [2], or by a new method, namely interference cancellation scheme [3]. The OFDM optimization on Rayleigh channel can also increase the capacity per user as shown in [4]. Therefore, OFDM has been widely used by several wireless communication standards, like digital video broadcasting-2nd generation terrestrial (DVB-T2) [5], microwave access (WiMAX) [6], long term evolution (LTE)/LTE-advanced (LTE-A) [7], optical wireless communication (OWC) [8], and one of the candidates for the 5th-generation (5G) standards [9].

The high peak-to-average power ratio (PAPR) is one-of the weaknesses of the OFDM system. This can be seen from the wide dynamic range of the symbol waveform. Precoding is used to improve the OFDM

system performance due to PAPR [10]. Apart from PAPR, errors in synchronization caused by radio frequency (RF) front-end non-idealities are another weakness of OFDM. The RF front-end non-idealities are usually caused due to imperfect manufacturing accuracy, communication channels, and component mismatches. This can cause symbol time offset (STO), in-phase and quadrature (IQ) imbalance, and carrier frequency offset (CFO), which will lead to inter-carrier interference (ICI) in OFDM system.

Like the conventional OFDM, precoded OFDM (P-OFDM) also has several disadvantages, including sensitivity to frequency offset, symbol timing error, and IQ imbalance. Precoded-OFDM using Walsh-Hadamard transform (WHT) performance has been evaluated and proven to improve energy and spectral efficiency in wireless communication systems [11]–[13]. The performance of P-OFDM was also evaluated in powerline communication with impulse noise [14], where the P-OFDM system excels the OFDM system in the respected scenarios.

Estimating CFO and IQ imbalance and investigating the impact on the OFDM system has been done by many researchers [15]–[25]. In previous studies, it was customary to measure the performance degradation resulting from CFO and IQ imbalance via bit error rates (BER) [15], [18], [20]–[22]. In [17], the average carrier to interference ratio (CIR_{QPSK}) is derived for OFDM with quadrature phase shift keying as data modulation, in case in the presence CFO and IQ imbalance. In [23], signal-to-interference noise ratio (SINR) analysis and performance evaluation in OFDM system in frequency-selective Rayleigh fading (FSRF) channel were carried out. The result is average SINR inversely proportional to RF-front-end non-idealities. In [24] performed a performance comparison between the OFDM and single-carrier with frequency-domain equalization (SC-FDE) systems due to CFO, IQ imbalance, and STO. The results are CFO induces a phase shift on SC-FDE system and ICI in OFDM system, whereas STO induces ISI on SC-FDE system and a phase shift in OFDM system. On the AWGN channel, the overall SC-FDE system is better than the OFDM system. Whereas in the FSRF channel, the SC-FDE system is more resistant to IQ imbalance while the OFDM system is more resistant to STO. In [25] studied the combined effects of RF non-idealities on a link-based mm-wave communication using OFDM system. As a result of RF non-idealities on the channel estimation in the form of carrier to interference ratio (CIR) is given. Particular attention should be given when using higher level of modulations, the use of low power, and low-cost RF transceivers in the mm-wave communications where ICI is one of the factors limiting its performance. Finally, in [26] evaluate the performance of P-OFDM in the present of CFO.

As indicated in the previous discussion, the impact of CFO and IQ imbalance has been widely studied. Nevertheless, with the best of the authors' knowledge, there is no open literature discussing the impact of CFO and IQ imbalance in the P-OFDM system where Walsh Hadamard transform (WHT) is used as a precoding transformation. In this study, the analysis of average SINR is given for P-OFDM in the additive white Gaussian noise (AWGN) channel and FSRF channel, as well as the simulation. The results of the analysis and simulation show that P-OFDM is greater affected than conventional OFDM with the presence of CFO and IQ imbalance. The SINR character in P-OFDM is different from conventional OFDM. In the AWGN channel, the SINR in P-OFDM is different for each subcarrier, while the OFDM is fixed. In the FSRF channel, the SINR fluctuations in the P-OFDM system are much larger than in the OFDM system. Therefore, although specific subcarriers are slightly affected by CFO and IQ imbalance, others will experience a severe decrease in SINR, which can decrease the overall BER. This causes the BER performance of P-OFDM to be inferior compare to conventional OFDM.

The remainder of this paper is arranged. In section 2 give out P-OFDM with CFO and IQ imbalance. Section 3 presents the average SINR expressions with CFO and IQ imbalance in AWGN channel and FSRF channel. The results and discussion are given in section 4. Lastly, section 5 provides the conclusion.

Notation: Vectors are represented by lower case bold letters and matrices are represented by upper case bold letters. The operator $|\cdot|$ and $\mathbb{E}[\cdot]$ stand for absolute value and expectation, respectively. Additionally, $(\cdot)^H$, $(\cdot)^T$, $(\cdot)^*$, $(\cdot)^{-1}$ denote Hermitian transposition, transpose operations, complex conjugate, inverse operations, respectively.

2. P-OFDM SYSTEM WITH CFO AND IQ IMBALANCE

The complex data symbols sent by the P-OFDM system can be represented as (1):

$$\mathbf{a} = \mathbf{W}\mathbf{d} \quad (1)$$

where $\mathbf{d} = [d_0, d_1, \dots, d_{N-1}]^T$ represents complex data symbols, \mathbf{W} represents WHT, and \mathbf{a} represents multiplication of \mathbf{W} and \mathbf{d} , respectively. The vector \mathbf{a} can be represented:

$$a_i = w_i d = \sum_{n=0}^{N-1} W_{i,n} d_n, \quad (2)$$

where w_i is the i -th row of the W matrix

$$w_i = [W_{i,0}, W_{i,1}, \dots, W_{i,N-1}] \quad (3)$$

$W_{i,n}$ represents the elements of the i -th row and n -th column of W , which is obtained from

$$W_{i,n} = \frac{1}{\sqrt{N}} (-1)^{\sum_{z=0}^{\log_2(N-1)} i_z n_z} \quad (4)$$

with i_z and n_z represent the bits of integer value of i and n . The time domain sample of vector a after the inverse fast Fourier transform (IFFT) process can be shown as (5):

$$x = F^H a \quad (5)$$

where F^H is the Hermitian transpose of the IFFT matrix with size $N \times N$. Each element of F^H is defined as $\frac{1}{\sqrt{N}} e^{j2\pi kn/N}$ where k and n denote the index of row and column $\{k, n\} \in 0, 1, \dots, N-1$. At the receiver, the received samples time domain vector (y) with a (CFO), can be expressed:

$$y = C(\xi) H F^H a \quad (6)$$

where H is the channel matrix with the number of multipath components L_h in the form of a circular matrix with size $N \times N$, where h_0 is on the main diagonal and $h_1 - h_{L_h-1}$ is on the minor diagonal. ξ is the normalization of CFO and $C(\xi)$ expresses the overall phase shift in the sample time-domain due to the normalization of CFO. So that $C(\xi)$ can be expressed:

$$C(\xi) = \text{diag}([e^{j2\pi\xi \times 0/N}, e^{j2\pi\xi \times 1/N}, \dots, e^{j2\pi\xi \times (N-1)/N}]) \quad (7)$$

Due to the IQ imbalance, the time domain \bar{y} row at the receiver can be expressed as (8) [15]:

$$\bar{y} = \alpha y + \beta y^* + \eta \quad (8)$$

where

$$\begin{aligned} \alpha &= \cos(q) + jQ \sin(q) \\ \beta &= Q \cos(q) - j\sin(q), \end{aligned} \quad (9)$$

with q denotes the phase imbalance and Q denotes the amplitude imbalance. The \bar{y} sequences after being processed by fast Fourier transform (FFT) can be expressed

$$r = F(\alpha C(\xi) H F^H a + \beta (C(\xi) H F^H a)^*) + \eta \quad (10)$$

$$r = S a + T a^* + \eta \quad (11)$$

where $S = \alpha F C(\xi) H F^H$, $T = \beta F C(\xi) H (F^H)^*$, the i -th element of r can be represented:

$$r_i = \alpha \sum_{p=0}^{N-1} S_{i,p} a_p + \beta \sum_{p=0}^{N-1} T_{i,p} a_p^* + \eta_i, \quad (12)$$

with $S_{i,p}$ and $T_{i,p}$ are the components of the i -th row and p -th column of S and T , which can be represented:

$$S_{i,p} = \frac{1}{N} \sum_{k=0}^{N-1} \sum_{l=0}^{L_h-1} h_l e^{j2\pi k(p-i+\xi)/N} e^{-j2\pi lp/N}, \quad (13)$$

$$T_{i,p} = \frac{1}{N} \sum_{k=0}^{N-1} \sum_{l=0}^{L_h-1} h_l e^{j2\pi k(i-p+\xi)/N} e^{j2\pi lp/N}. \quad (14)$$

After being manipulated, (13) and (14) can be written

$$S_{i,p} = f_{i,p} H_p \quad (15)$$

$$T_{i,p} = g_{i,p} H_p^* \quad (16)$$

where $H_p = \sum_{l=0}^{L_h-1} h_l e^{-j2\pi lp/N}$,

$$f_{i,p} = \frac{\sin(\pi((p-i+\xi)))}{N \sin(\frac{\pi}{N}((p-i+\xi)))} \quad (17)$$

and

$$g_{i,p} = \frac{\sin(\pi((i-p+\xi)))}{N \sin(\frac{\pi}{N}((i-p+\xi)))} \quad (18)$$

The data elements at the receiver after the inverse W process are

$$\begin{aligned} \hat{d}_k &= W_k^{-1} \mathbf{r} \\ &= \sum_{i=0}^{N-1} W_{k,i}^{-1} T_i \\ &= \alpha \sum_{i=0}^{N-1} \sum_{p=0}^{N-1} W_{k,i}^{-1} S_{i,p} d_p + \beta \sum_{i=0}^{N-1} \sum_{p=0}^{N-1} W_{k,i}^{-1} T_{i,p} d_p^* + \omega_k \end{aligned} \quad (19)$$

$$\hat{d}_k = \alpha \gamma_{k,k} d_k + \alpha \sum_{\substack{n=0 \\ n \neq k}}^{N-1} \gamma_{k,n} d_n + \beta \sum_{n=0}^{N-1} \delta_{k,n} d_n^* + \omega_k \quad (20)$$

where $\omega_k = \sum_{i=0}^{N-1} W_{k,i}^{-1} \eta_i$

$$\gamma_{k,n} = \sum_{i=0}^{N-1} \sum_{p=0}^{N-1} W_{k,i}^{-1} W_{p,n} S_{i,p} \quad (21)$$

and

$$\delta_{k,n} = \sum_{i=0}^{N-1} \sum_{p=0}^{N-1} W_{k,i}^{-1} W_{p,n} T_{i,p} \quad (22)$$

3. SINR ANALYSIS OF P-OFDM

Regarding on (20), the average SINR for the k -th subcarrier can be expressed:

$$\overline{\text{SINR}}_k = \frac{\mathbb{E}[|\alpha \gamma_{k,k} d_k|^2]}{\mathbb{E}\left[\left| \alpha \sum_{\substack{n=0 \\ n \neq k}}^{N-1} \gamma_{k,n} d_n \right|^2 \right] + \mathbb{E}\left[\left| \beta \sum_{n=0}^{N-1} \delta_{k,n} d_n^* \right|^2 \right] + \sigma_{\omega_k}^2} \quad (23)$$

The equation (23) can be rewritten as (assuming d_n and d_n^* have the same average power, i.e. P_s)

$$\overline{\text{SINR}}_k = \frac{\mathbb{E}[|\alpha \gamma_{k,k}|^2]}{\mathbb{E}\left[\left| \alpha \sum_{\substack{n=0 \\ n \neq k}}^{N-1} \gamma_{k,n} \right|^2 \right] + \mathbb{E}\left[\left| \beta \sum_{n=0}^{N-1} \delta_{k,n} \right|^2 \right] + \sigma_{\omega_k}^2} \quad (24)$$

For the AWGN case where $H_p = 1$ for all p . Therefore (24) can be reduced to

$$\overline{\text{SINR}}_k = \frac{|\alpha|^2 \left| \sum_{i=0}^{N-1} \sum_{p=0}^{N-1} W_{k,i}^{-1} W_{p,k} f_{i,p} \right|^2}{|\alpha|^2 \sum_{\substack{n=0 \\ n \neq k}}^{N-1} \left| \sum_{i=0}^{N-1} \sum_{p=0}^{N-1} W_{k,i}^{-1} W_{p,n} f_{i,p} \right|^2 + |\beta|^2 \sum_{n=0}^{N-1} \left| \sum_{i=0}^{N-1} \sum_{p=0}^{N-1} W_{k,i}^{-1} W_{p,n} g_{i,p} \right|^2 + \sigma_{\omega_k}^2} \quad (25)$$

Furthermore, the output of the inverse WHT at the receiver can be represented in (26):

$$\begin{aligned} \hat{\mathbf{d}} &= \mathbf{W}^{-1} \mathbf{H}^{-1} \mathbf{F} (\alpha \mathbf{C}(\xi) \mathbf{H} \mathbf{F}^H \mathbf{a} + \beta (\mathbf{C}(\xi) \mathbf{H} \mathbf{F}^H \mathbf{a})^*) + \boldsymbol{\eta} \\ &= \mathbf{G} \mathbf{d} + \mathbf{K} \mathbf{d}^* + \boldsymbol{\omega} \end{aligned} \quad (26)$$

where $\omega = [\omega_0, \omega_{1,\dots}, \omega_{N-1}]^T$, G, and K as in (27), and (28), respectively.

$$G = \begin{bmatrix} S_{0,0} & 0 & 0 & 0 & 0 & 0 & 0 & 0 \\ 0 & S_{1,1} & 0 & 0 & 0 & 0 & 0 & 0 \\ 0 & 0 & S_{2,2} & S_{2,3} & 0 & 0 & 0 & 0 \\ 0 & 0 & S_{3,2} & S_{3,3} & 0 & 0 & 0 & 0 \\ \vdots & \vdots & \vdots & \vdots & \ddots & 0 & 0 & 0 \\ 0 & 0 & 0 & 0 & S_{\frac{N}{2}, \frac{N}{2}} & S_{\frac{N}{2}, \frac{N}{2}+1} & \dots & S_{\frac{N}{2}, N-1} \\ 0 & 0 & 0 & 0 & S_{\frac{N}{2}+1, \frac{N}{2}} & S_{\frac{N}{2}+1, \frac{N}{2}+1} & \dots & S_{\frac{N}{2}+1, N-1} \\ 0 & 0 & 0 & 0 & \vdots & \vdots & \vdots & \vdots \\ 0 & 0 & 0 & 0 & S_{N-1, \frac{N}{2}} & S_{N-1, \frac{N}{2}+1} & \dots & S_{N-1, N-1} \end{bmatrix} \quad (27)$$

$$K = \begin{bmatrix} T_{0,0} & 0 & 0 & 0 & 0 & 0 & 0 & 0 \\ 0 & T_{1,1} & 0 & 0 & 0 & 0 & 0 & 0 \\ 0 & 0 & T_{2,2} & T_{2,3} & 0 & 0 & 0 & 0 \\ 0 & 0 & T_{3,2} & T_{3,3} & 0 & 0 & 0 & 0 \\ \vdots & \vdots & \vdots & \vdots & \ddots & 0 & 0 & 0 \\ 0 & 0 & 0 & 0 & T_{\frac{N}{2}, \frac{N}{2}} & T_{\frac{N}{2}, \frac{N}{2}+1} & \dots & T_{\frac{N}{2}, N-1} \\ 0 & 0 & 0 & 0 & T_{\frac{N}{2}+1, \frac{N}{2}} & T_{\frac{N}{2}+1, \frac{N}{2}+1} & \dots & T_{\frac{N}{2}+1, N-1} \\ 0 & 0 & 0 & 0 & \vdots & \vdots & \vdots & \vdots \\ 0 & 0 & 0 & 0 & T_{N-1, \frac{N}{2}} & T_{N-1, \frac{N}{2}+1} & \dots & T_{N-1, N-1} \end{bmatrix} \quad (28)$$

By referring to the block matrices G and K, it is shown that the impact of CFO and IQ on each subcarrier is different, some are minimal and some are severe. For example, the subcarrier that has minimal impact is the subcarrier $\hat{d}_0 = S_{0,0}d_0 + T_{0,0}d_0^* + \omega_0$ where the attenuation factor is $S_{0,0}$ and the interference factor is $T_{0,0}d_0^*$. While the subcarrier that experienced severe impact is the subcarrier $\hat{d}_2 = S_{2,2}d_2 + S_{2,3}d_2 + T_{2,2}d_2^*d_2 + T_{2,3}d_2^* + \omega_2$, where the attenuation factor is $S_{2,2}$ and the interference factor is $S_{2,3}d_2 + T_{2,2}d_2^*d_2 + T_{2,3}d_2^*$. This causes SINR of $\hat{d}_0 > \text{SINR}$ of \hat{d}_2 .

4. RESULTS AND DISCUSSION

In this section, we present the simulation results of the P-OFDM system on the AWGN channel and the FSRF channel. For the FSRF channel used in this simulation, it has 6 paths with a delay of [0, 1, 3, 5, 7, 10] samples and the average gain for each path is [0.6, 0.32, 0.16, 0.11, 0.08, 0.04]. Table 1 shows the overall simulation of the parameters. Perfect channel knowledge and Zero-Forcing equalization have been assumed.

Table 1. The parameters of simulation scenario

No.	Parameters	Values
1.	Number of FFT point	$N = 256$
2.	Subcarrier spacing	15 khz
3.	OFDM symbol duration (T_u)	$T_u = 66.68 \mu s$
4.	Total OFDM symbol duration (T_t)	$T_t = 75.015 \mu s$
5.	Number of CP	$N/8$
6.	Data modulation	4-QAM (quadrature amplitude modulation)

Figure 1 shows the $\overline{\text{SINR}}_k$ to the subcarrier index for the AWGN channel and Figure 2 shows the $\overline{\text{SINR}}_k$ to the subcarrier index for the FSRF channel. In both simulations, SNR=20 dB and $\xi = 0.1$ are used. In the AWGN channel as shown in Figure 1, the SINR for all subcarriers of the OFDM is identical, while in the P-OFDM the SINR is a function of the subcarrier index. In the FSRF channel as shown in Figure 2, the SINR in OFDM is not the same for each subcarrier, this is due to the effect of channel compensation on the signal with residuals from CFO and IQ imbalance. The same thing happens to the P-OFDM signal, where the SINR is a function of the subcarrier index with a lower value than the SINR in the AWGN channel. From these results, it is shown that the presence of CFO and IQ imbalance can cause a more severe reduction in

BER in the case of P-OFDM, which the entire BER system is likely to come mostly from subcarriers with low SINRs.

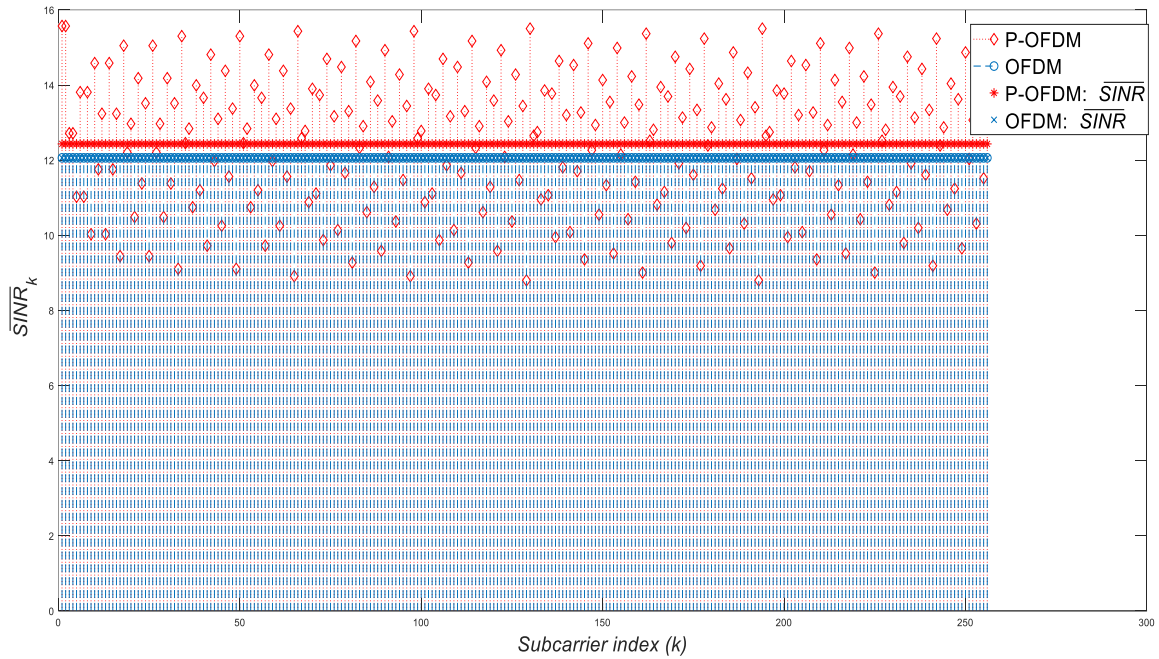


Figure 1. Simulated SINR per subcarrier of P-OFDM and OFDM for AWGN channel

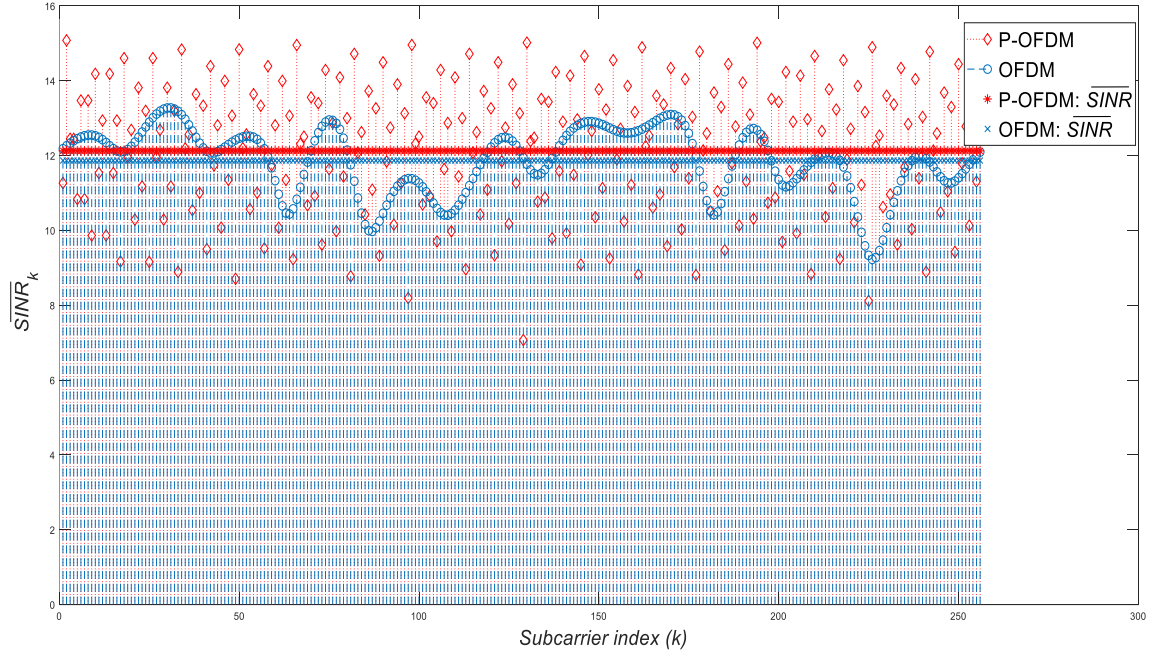


Figure 2. Simulated SINR per subcarrier of P-OFDM and OFDM for FSRF channel

The simulation results for $\xi = 0.1$, $Q = 0.1$, and $q = 5^\circ$ are shown in Figure 3 for the AWGN channel and Figure 4 for the FSRF channel. In the AWGN channel, it is shown that each subcarrier in the P-OFDM system has different interference, so some subcarriers have a higher BER performance than other subcarriers. This is because each subcarrier experiences a different level of interference. This is in

accordance with what is described in Figure 1. This is different from the OFDM system, where each subcarrier experiences almost the same level of interference. In the FSRF channel, the two systems experience different levels of interference for each subcarrier. This is in accordance with what is described in Figure 2, where the channel equalization process is disrupted due to CFO and IQ imbalance.

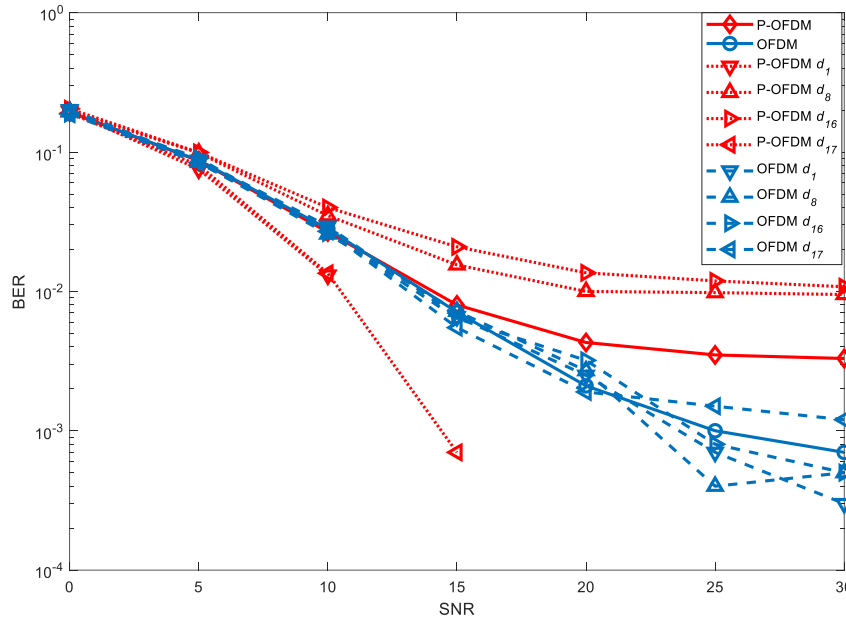


Figure 3. Simulated average SINR of P-OFDM and OFDM for AWGN channel

The simulation results of P-OFDM and OFDM under ideal RF conditions (CFO=0 and IQ=0) are depicted in Figure 5. On the AWGN channel, the performance of P-OFDM is almost the same as that of OFDM, but in the FSRF channel, the performance of P-OFDM is slightly decreased, especially at low SNR. This is because the channel equalization under high noise conditions is coupled with the overall BER system, which is likely to be dominated by subcarriers with low SINRs.

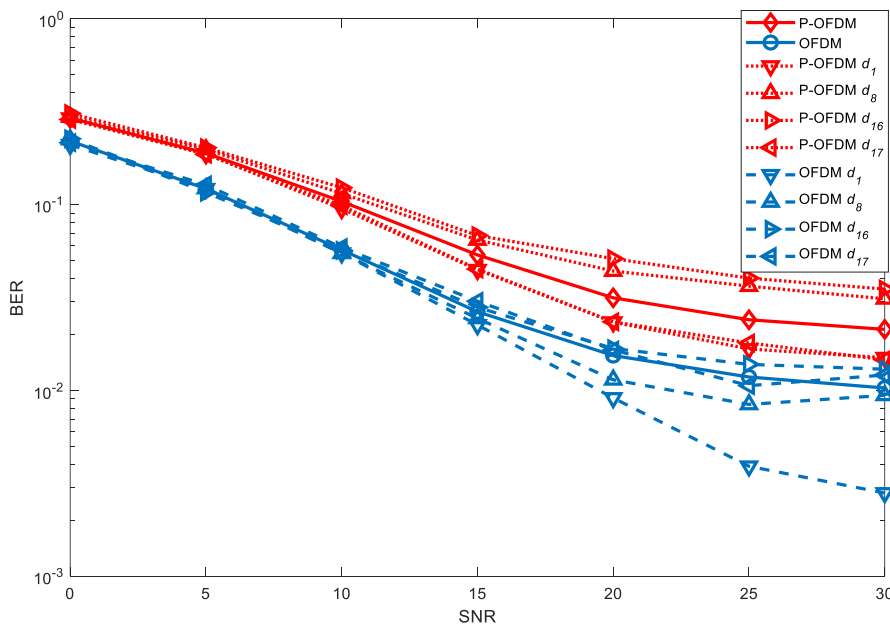


Figure 4. Simulated average SINR of P-OFDM and OFDM for FSRF channel

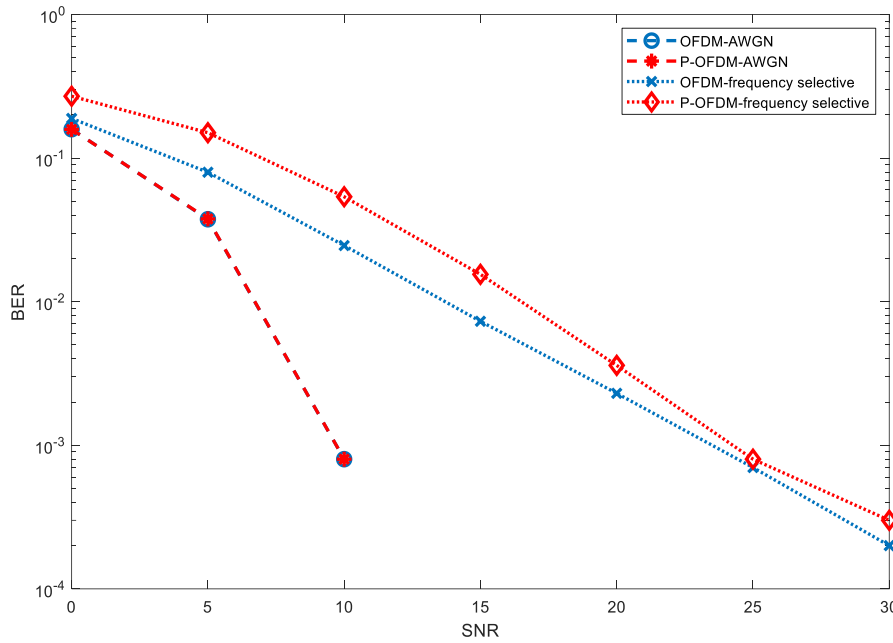


Figure 5. BER versus SNR for P-OFDM and OFDM under AWGN channel and FSRF channel

The simulation results ($Q = 0.05, Q = 0.1, q = 5^\circ, \text{ and } q = 10^\circ$) are shown in Figure 6 for $\xi = 0.05$ and Figure 7 for $\xi = 0.1$. It can be seen that the higher the CFO and IQ, the lower the performance of the two systems, both on the AWGN channel and the FSRF channel. P-OFDM performance on the AWGN channel is slightly decreased when compared to the conventional OFDM system. This also applies to FSRF channel, where P-OFDM performance decreases with increasing CFO and IQ imbalance. This is because the SINRs in P-OFDM fluctuate higher when compared to SINRs in OFDM, which causes the overall system BER to be lower.

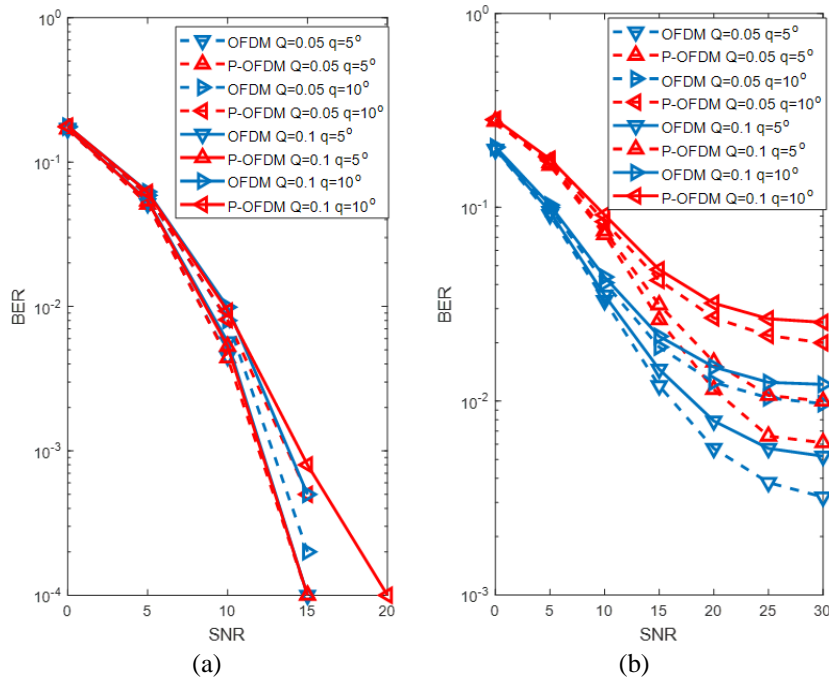


Figure 6. Simulated BER for P-OFDM and OFDM with $\xi = 0.05$ under (a) AWGN channel and (b) FSRF channel

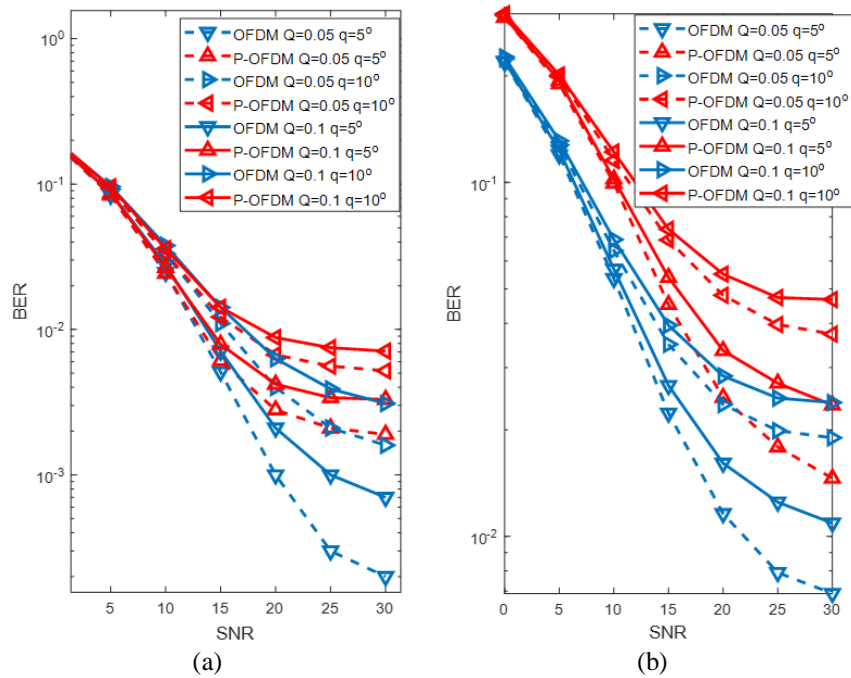


Figure 7. Simulated BER for P-OFDM and OFDM with $\xi = 0.1$ under (a) AWGN channel and (b) FSRF channel

5. CONCLUSION

In this paper, the impact of CFO and IQ imbalance on the WHT-based P-OFDM system is analyzed for its performance in the form of BER, where the OFDM system is used as a comparison. The average SINR in the P-OFDM system was evaluated in the AWGN channel and the FSRF channel. The SINR_k expression was derived and analyzed for the AWGN channel and the FSRF channel. Simulations are provided to validate our analysis. From our simulation results can be seen that the P-OFDM system experiences different interference in each subcarrier due to CFO and IQ imbalance. Mitigation of bit loading on individual subcarriers can be done to reduce the overall BER.

ACKNOWLEDGEMENTS

We would like to thank to the editor and the reviewers for their comments and suggestions, and also to the Indonesia Endowment Fund for Education (LPDP) and *Rumah Program Kendaraan Listrik* or IPT BRIN for their support.

REFERENCES

- [1] Y. Mostofi and D. C. Cox, "Robust timing synchronization design in OFDM systems-Part II: high-mobility cases," *IEEE Transactions on Wireless Communications*, vol. 6, no. 12, pp. 4340–4348, Dec. 2007, doi: 10.1109/TWC.2007.05901.
- [2] S. Suyoto, I. Iskandar, S. Sugihartono, and A. Kurniawan, "Improved timing estimation using iterative normalization technique for OFDM systems," *International Journal of Electrical and Computer Engineering (IJECE)*, vol. 7, no. 2, pp. 905–911, Apr. 2017, doi: 10.11591/ijece.v7i2.pp905-911.
- [3] X. Liu, H.-H. Chen, W. Meng, and B.-Y. Lyu, "Successive multipath interference cancellation for CP-free OFDM systems," *IEEE Systems Journal*, vol. 13, no. 2, pp. 1125–1134, Jun. 2019, doi: 10.1109/JSYST.2018.2838663.
- [4] P. Varzakas, "Optimization of an OFDM Rayleigh fading system," *International Journal of Communication Systems*, vol. 20, no. 1, pp. 1–7, Jan. 2007, doi: 10.1002/dac.807.
- [5] A. Omri, R. Hamila, A. Hazmi, R. Bouallegue, and A. Al-Dweik, "Enhanced Alamouti decoding scheme for DVB-T2 systems in SFN channels," in *2011 IEEE 22nd International Symposium on Personal, Indoor and Mobile Radio Communications*, Sep. 2011, pp. 1626–1630, doi: 10.1109/PIMRC.2011.6139779.
- [6] J. G. Andrews, A. Ghosh, and R. Muhamed, "Fundamentals of WiMAX." Prentice Hall, 2007.
- [7] E. Dahlman, S. Parkvall, and J. Sköld, *4G: LTE/LTE-advanced for mobile broadband*. Academic Press, 2011.
- [8] N. J. Jihad and S. M. Abdul Satar, "BER performance study for optical OFDM of optical camera communication," *International Journal of Electrical and Computer Engineering (IJECE)*, vol. 11, no. 5, pp. 4263–4271, Oct. 2021, doi: 10.11591/ijece.v11i5.pp4263-4271.
- [9] J. G. Andrews et al., "What will 5G be?," *IEEE Journal on Selected Areas in Communications*, vol. 32, no. 6, pp. 1065–1082, Jun. 2014, doi: 10.1109/JSAC.2014.2328098.
- [10] J. Mountassir, A. Isar, and T. Mountassir, "Precoding techniques in OFDM systems for PAPR reduction," in *2012 16th IEEE*

Impact of carrier frequency offset and in-phase and quadrature imbalance on the performance of ... (Suyoto)

- Mediterranean Electrotechnical Conference*, Mar. 2012, pp. 728–731, doi: 10.1109/MELCON.2012.6196534.
- [11] F. Kalbat, A. Al-Dweik, B. Sharif, and G. Karagiannidis, “Robust precoded MIMO-OFDM for mobile frequency-selective wireless channels,” in *2016 IEEE Wireless Communications and Networking Conference*, Apr. 2016, pp. 1–6, doi: 10.1109/WCNC.2016.7564880.
- [12] S. Wang, S. Zhu, and G. Zhang, “A Walsh-Hadamard coded spectral efficient full frequency diversity OFDM system,” *IEEE Transactions on Communications*, vol. 58, no. 1, pp. 28–34, Jan. 2010, doi: 10.1109/TCOMM.2010.01.070605.
- [13] M. S. Ahmed, S. Boussakta, B. S. Sharif, and C. C. Tsimenidis, “OFDM based on low complexity transform to increase multipath resilience and reduce PAPR,” *IEEE Transactions on Signal Processing*, vol. 59, no. 12, pp. 5994–6007, Dec. 2011, doi: 10.1109/TSP.2011.2166551.
- [14] A. Khan and S. Y. Shin, “Linear precoded wavelet OFDM-based PLC system with overlap FDE for impulse noise mitigation,” *International Journal of Communication Systems*, vol. 30, no. 17, Nov. 2017, doi: 10.1002/dac.3349.
- [15] J. Tubbx *et al.*, “Joint compensation of IQ imbalance and frequency offset in OFDM systems,” in *Radio and Wireless Conference, 2003. RAWCON '03. Proceedings, 2003*, pp. 39–42, doi: 10.1109/RAWCON.2003.1227887.
- [16] J.-Y. Yu, M.-F. Sun, T.-Y. Hsu, and C.-Y. Lee, “A novel technique for I/Q imbalance and CFO compensation in OFDM systems,” in *2005 IEEE International Symposium on Circuits and Systems*, 2005, pp. 6030–6033, doi: 10.1109/ISCAS.2005.1466014.
- [17] G. Xing, M. Shen, and H. Liu, “Frequency offset and I/Q imbalance compensation for OFDM direct-conversion receivers,” in *2003 IEEE International Conference on Acoustics, Speech, and Signal Processing, 2003. Proceedings. (ICASSP '03)*, 2003, vol. 4, pp. IV--708--11, doi: 10.1109/ICASSP.2003.1202741.
- [18] I. Barhum and M. Moonen, “IQ-imbalance compensation for OFDM in the presence of IBI and carrier-frequency offset,” *IEEE Transactions on Signal Processing*, vol. 55, no. 1, pp. 256–266, Jan. 2007, doi: 10.1109/TSP.2006.882102.
- [19] C. Ma, G. E. Atkin, and C. Zhou, “Variable sub-carrier in OFDM to reduce the ICI due to carrier frequency offset and IQ imbalance,” in *Third IEEE International Conference on Wireless and Mobile Computing, Networking and Communications (WiMob 2007)*, Oct. 2007, p. 12, doi: 10.1109/WIMOB.2007.4390806.
- [20] F. Horlin, A. Bourdoux, and L. Van Der Perre, “Low-complexity EM-based joint acquisition of the carrier frequency offset and IQ imbalance,” *IEEE Transactions on Wireless Communications*, vol. 7, no. 6, pp. 2212–2220, Jun. 2008, doi: 10.1109/TWC.2008.060954.
- [21] J.-R. Liang and C.-H. Kuo, “LS-based joint estimation of carrier frequency offset and IQ imbalance in OFDM systems,” in *2010 International Symposium on Next Generation Electronics*, Nov. 2010, pp. 52–55, doi: 10.1109/ISNE.2010.5669203.
- [22] M.-W. Wen, X. Cheng, X. Wei, B. Ai, and B.-L. Jiao, “A novel effective ICI self-cancellation method,” in *2011 IEEE Global Telecommunications Conference-GLOBECOM 2011*, Dec. 2011, pp. 1–5, doi: 10.1109/GLOCOM.2011.6133714.
- [23] R. Zhang, E. K. S. Au, and R. S. Cheng, “Impacts of CFO, IQ imbalance and phase noise on the system performance in OFDM systems,” in *2008 11th IEEE Singapore International Conference on Communication Systems*, Nov. 2008, pp. 1041–1045, doi: 10.1109/ICCS.2008.4737341.
- [24] F. Horlin and A. Bourdoux, “Comparison of the sensitivity of OFDM and SC-FDE to CFO, SCO and IQ imbalance,” in *2008 3rd International Symposium on Communications, Control and Signal Processing*, Mar. 2008, pp. 111–116, doi: 10.1109/ISCCSP.2008.4537202.
- [25] Y. Zou *et al.*, “Impact of major RF impairments on mm-wave communications using OFDM waveforms,” in *2016 IEEE Globecom Workshops (GC Wkshps)*, Dec. 2016, pp. 1–7, doi: 10.1109/GLOCOMW.2016.7848927.
- [26] F. Kalbat, A. Al-Dweik, B. Sharif, and G. K. Karagiannidis, “Performance analysis of precoded wireless OFDM with carrier frequency offset,” *IEEE Systems Journal*, vol. 14, no. 2, pp. 2237–2248, Jun. 2020, doi: 10.1109/JSYST.2019.2922098.

BIOGRAPHIES OF AUTHORS



Suyoto    is currently a researcher at Research Center Electronics and Telecommunication National Research and Innovation Agency (BRIN). Obtained Bachelor of Telecommunication Engineering, Master in Computer and Multimedia Systems, and Doctor of Telecommunication Engineering all from the Bandung Institute of Technology in 2002, 2009 and 2019, respectively. His research interests include signal processing, synchronization, multicarrier system, and wireless communication. He can be contacted at email: suyotofx@gmail.com.



Agus Subekti    got bachelor and master degree in electrical engineering from Bandung Institute of Technology, Indonesia, in 1998 and 2001 respectively. He finished his Ph.D. in electrical engineering and informatics from Bandung Institute of Technology (ITB), in 2016. He was a research associate at Nakajima Laboratory, Tokai University, Japan in 2002-2004. Currently, he is a researcher with National Research and Innovation Agency since 2005. He can be contacted at email: agus.subekti76@gmail.com.



Arief Suryadi Satyawan    has joined with Research Center for Electronics and Telecommunication, National Research and Innovation Agency, since 1996. He received his Bachelor's degree in electrical engineering from Universitas Jenderal Achmad Yani Bandung, Indonesia, in 2000. In 2007, he received his Master's degree in electrical engineering from Institut Teknologi Bandung, Indonesia. He got his Ph.D. in computer and communication engineering from Waseda University, Japan, in 2019. His current research is image and video processing, and video communication system. He is a member of The Institute of Image Information and Television Engineers (ITE), Japan, and Information Processing Society of Japan (IPSJ). He can be contacted at email: arief.suryadi@akane.waseda.jp.



Nasrullah Armi    received Master Degree from Department of Knowledge based Information Engineering, Toyohashi University of Technology, Japan in 2004. Subsequently, he obtained his Ph.D. degree from Department of Electrical and Electronic Engineering, Universiti Teknologi Petronas, Malaysia in 2013. His research interests are Signal Processing, Wireless Communication and Networks. He published scientific articles on peer review journals and participated on international conferences. He contributed his knowledge as scientific reviewer in international impact journals and became Scientific Committee in International Conferences. Currently, he is working as a researcher at National Research and Innovation Agency, Research Center for Electronics and Telecommunication. He can be contacted at email: Nasrullah.armi@gmail.com.



Chaeriah Ali Wael    is currently working as junior researcher at the Research Center for Electronics and Telecommunications, National Research and Innovation Agency. Her research interests lie in the area of signal processing, communication and information theory with a focus on Physical and MAC layer issues including modulation techniques, coding, equalization and synchronization, signal detection and estimation, cooperative communication, radio resource management, cognitive radio and spectrum optimization techniques. She can be contacted at email: chaeriah.wael10@gmail.com.



Galih Nugraha Nurkahfi    is currently a researcher at Research Center Electronics and Telecommunication National Research and Innovation Agency (BRIN). Obtained Bachelor of Physics, Master in Telecommunication Engineering all from the Bandung Institute of Technology in 2008 and 2016 respectively. His research interest includes telematics, computer network, wireless telecommunication, data, and IoT. He can be contacted at email: galih004@lipi.go.id.